rests on the Pacific plate (Fig. 3), and the interface between them plays the role of the main thrust zone (that is, there is no slip on the surface) during the strain accumulation interval. The ultimate rupture, however, does not follow that interface all the way to the trailing edge of the Yakutat block but rather breaks upward through the block (*12*) along one or more of the listric, imbricate thrust faults between the Pamplona fault zone and the Chugach–St. Elias fault (Fig. 3). A model for subduction and collision in the Yakataga gap and the associated strain rate ($\dot{\epsilon}_{22}$) profile is shown in Fig. 3. The down-dip end of the main thrust zone in that model is located at a change in dip in the plate interface inferred from seismicity (*13*). The model predicts a rate of strain accumulation across the Yakataga trilateration network with $\dot{\epsilon}_{22}$ equal to -0.15 μstrain per year and $\dot{\epsilon}_{11}$ and $\dot{\epsilon}_{12}$ both equal to zero. The equivalent shear strain rates are $\dot{\gamma}_1 = 0.15$ μrad/year and $\dot{\gamma}_2 = 0$. The observed value of $\dot{\gamma}_1$ (0.26 ± 0.05 μrad/year) is somewhat larger than predicted but is within the range that could be accounted for by movement of the north end of the main thrust zone up-dip. The observed value of $\dot{\gamma}_2$ (0.19 ± 0.04 μrad/year) indicates a right-lateral transverse shear not predicted by the model. This transverse shear may indicate that the plate convergence in the Yakataga gap is more oblique than suggested by the N15°W direction given by the model of Minster and Jordan (*7*). A more oblique convergence is supported by the coincidence between the N38°W direction of maximum compression and the N37°W strike of the Fairweather fault (locus of the 1958 rupture in Fig. 1), which is the right-slip transform that forms the lateral, North American–Pacific plate boundary in southeastern Alaska. This oblique convergence may be a product of slip-line flow (*14*) in which the Yakutat plate is squeezed to the west. In any case we are satisfied that strain is accumulating in the Yakataga gap at a rate commensurate with the eventual occurrence of a great plate-margin earthquake.

REFERENCES AND NOTES

1. J. Davies, L. Sykes, L. House, K. Jacob, *J. Geophys. Res.* **86**, 3821 (1981).
2. W. R. McCann, O. J. Pérez, L. R. Sykes, *Science* **207**, 1309 (1980). A small portion of the Yakataga gap did rupture in the 1979 St. Elias earthquake (Fig. 1) (see J. C. Lahr, C. D. Stephens, H. S. Hasegawa, J. Boatwright, *ibid.*, p. 1351).
3. K. H. Jacob, *Geophys. Res. Lett.* **11**, 295 (1984).
4. J. C. Savage and W. H. Prescott, *J. Geophys. Res.* **78**, 6001 (1973).
5. Systematic errors in trilateration tend to appear as proportional errors in line length (for example, all lines too short by 0.5 ppm). In calculating strain, such systematic errors are indistinguishable from an isotropic extension. Thus, a systematic error will appear directly in the tensor extensions ϵ_{11} and ϵ_{22} and in double proportion in the areal dilatation Δ. Because the shear components are the differences between two orthogonal extensions, those components are relatively free of proportional error. In our measurements, the error in measuring a line is composed of about equal parts random and systematic error. In calculating strain the random errors from the redundant observations tend to cancel, so that systematic error becomes dominant [see J. C. Savage, W. H. Prescott, M. Lisowski, N. E. King, *ibid.* **86**, 6991 (1981)].
6. J. C. Savage, *ibid.* **88**, 4984 (1983). A critical element in calculating the deformation rates is the particular earth model used. We have used an elastic half-space representation. That model yields the time-averaged deformation over the entire interseismic interval. A more complicated model that includes representation of a viscoelastic asthenosphere yields a time-dependent deformation in which the more rapid rates occur early in the cycle [see W. Thatcher and J. B. Rundle, *ibid.* **89**, 7631 (1984)].
7. J. B. Minster and T. H. Jordan, *ibid.* **83**, 5331 (1978).
8. M. Reyners and K. S. Coles, *ibid.* **87**, 356 (1983).
9. K. Nakane, *J. Geodetic Soc. Japan* **19**, 200 (1973).
10. J. Beavan, E. Haukssón, S. R. McNutt, R. Bilham, K. H. Jacob, *Science* **222**, 322 (1983); J. Beavan, R. Bilham, K. Hurst, *J. Geophys. Res.* **89**, 4478 (1984).
11. J. C. Lahr and G. Plafker, *Geology* **8**, 483 (1980); T. R. Bruns, *ibid.* **11**, 718 (1983).
12. O. J. Perez and K. H. Jacob, *J. Geophys. Res.* **85**, 7141 (Figure 4a) (1980).
13. C. D. Stephens, K. A. Fogelman, J. C. Lahr, R. A. Page, *Geology* **12**, 373 (1984).
14. P. Tapponnier and P. Molnar, *Nature (London)* **264**, 319 (1976).
15. L. R. Sykes, J. B. Kisslinger, L. House, J. N. Davies, K. H. Jacob, in *Proceedings of the Fourth Ewing Symosium* (American Geophysical Union, Washington, DC, 1981), pp. 73–79.
16. H. Kanamori, *J. Geophys. Res.* **82**, 2981 (1977).

5 August 1985; accepted 16 October 1985

Translocation of Protein Kinase C Activity May Mediate Hippocampal Long-Term Potentiation

RAYMOND F. AKERS, DAVID M. LOVINGER, PATRICIA A. COLLEY, DAVID J. LINDEN, ARYEH ROUTTENBERG*

Protein kinase C activity in rat hippocampal membranes and cytosol was determined 1 minute and 1 hour after induction of the synaptic plasticity of long-term potentiation. At 1 hour after long-term potentiation, but not at 1 minute, protein kinase C activity was increased twofold in membranes and decreased proportionately in cytosol, suggesting translocation of the activity. This time-dependent redistribution of enzyme activity was directly related to the persistence of synaptic plasticity, suggesting a novel mechanism regulating the strength of synaptic transmission.

PROTEIN KINASE ACTIVATION LEADING to phosphorylation of neural proteins appears to occupy a pivotal role in the development and expression of synaptic plasticity (*1*). We have suggested that the activation of Ca^{2+}-phospholipid–dependent protein kinase C (PKC) and the phosphorylation of one of its substrates, protein F1, represents a key step in the expression of synaptic plasticity (*2*). This proposal is based on evidence that long-term potentiation (LTP), a persistent enhancement of hippocampal synaptic efficacy, elevates the in vitro phosphorylation of protein F1 (*3*), a 47K, synaptically enriched phosphoprotein (*p*I, 4.5) (*4*). This increase in F1 phosphorylation persisted for 3 days after the induction of LTP and was directly related to the persistence of the change in synaptic efficacy (*5*).

Since protein F1 is a PKC substrate (*6, 7*), LTP could activate PKC in vivo (*6*). Protein kinase C is activated in vitro by phosphatidylserine and diacylglycerol in the presence of Ca^{2+} (*8*). However, due to the rapid breakdown of diacylglycerol after receptor activation (*9*), it is unlikely that diacylglycerol formation could account for a more prolonged activation of PKC, as would be required to maintain the long-term elevation of protein F1 phosphorylation after LTP. This prolonged activation might result from a redistribution of PKC from cytosol to membranes, similar to the strong attachment of PKC to membranes produced by the tumor-promoting phorbol esters (*10, 11*). Such a stable attachment could account for an extended period of enzyme activation necessary for the maintenance of elevated F1 phosphorylation levels during long-term plasticity. Accordingly, we determined whether the synaptic plasticity of LTP would result in the translocation of PKC activity to membranes.

Male albino rats were anesthetized with urethane and stimulating electrodes were placed in the perforant path, the axonal system that connects the entorhinal cortex with the dentate gyrus. A single recording electrode was placed in several different dorsal hippocampal positions to define the extent of synaptic invasion elicited by perfor-

Cresap Neuroscience Laboratory, Northwestern University, Evanston, IL 60201.

*To whom correspondence should be addressed.

Fig. 1. Increase in PKC activity in membranes 1 hour after LTP. The extent of perforant path activation of the dentate gyrus in male albino rats was first determined. High-frequency repetitive stimulation (eight trains of eight 100-Hz pulses) or low-frequency control stimulation (64 pulses at 0.1 Hz) was then delivered. One minute or 1 hour later the animals were killed by rapid freezing in liquid nitrogen. The innervated regions of the dorsal hippocampus were dissected on a block of dry ice and homogenized in 50 m*M* tris (*p*H 7.2), 0.1 m*M* EDTA, and leupeptin (10 μg/ml). To obtain particulate and soluble fractions for each dorsal hippocampus, homogenates were spun at 100,000*g* for 1 hour and the resulting supernatants were collected. The pellets were washed and the supernatants were combined. The supernatants, containing PKC activity from the cytosolic fraction, were then applied to a 0.4 by 1.0 cm DEAE-cellulose column equilibrated with 50 m*M* tris (*p*H 7.2), 2 m*M* EGTA, and 2 m*M* EDTA. After sample addition, the columns were washed with 2 ml of equilibration buffer and PKC activity was eluted with 400 μl of 0.3*M* NaCl. To obtain particulate PKC activity, the 100,000*g* pellet was resuspended in 50 m*M* tris (*p*H 7.2), 0.1 percent Triton X-100, 2 m*M* EDTA, 2 m*M* EGTA, and leupeptin (10 μg/ml), and the mixture was stirred for 1 hour at 4°C. After centrifugation at 100,000*g* for 1 hour to remove debris, the supernatants, containing PKC activity extracted from membranes, were applied to DEAE-cellulose columns and PKC activity was eluted as before. PKC activity was determined in the following assay mix: 50 m*M* tris (*p*H 7.2), 1.5 m*M* $CaCl_2$, 0.5 m*M* EGTA, 0.5 m*M* EDTA, 100 μg of histone H1, 3 to 5 μg of enzyme preparation, and 0.5 m*M* [γ-^{32}P]ATP (specific activity, 50 cpm/pmol), with or without phosphatidylserine (100 μg/ml). The reaction was run for 10 minutes at 30°C, quenched with a saturated EDTA solution, and spotted onto phosphocellulose paper. The papers were washed and radioactivity was counted by liquid scintillation spectrometry. PKC activity was taken as the difference between activity seen in the presence or absence of phosphatidylserine. All enzyme assays were linear with respect to time and enzyme concentration. Values are means ± standard errors (only the −standard error is shown; $n = 6$ for all groups except controls, where $n = 7$); Student's *t*-test was used for calculating probability.

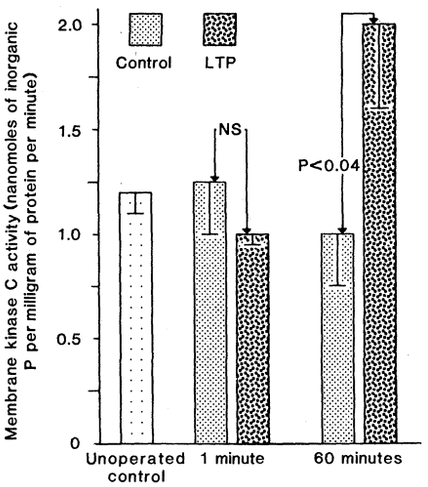

ant path stimulation (*2*). High-frequency (400 Hz) repetitive stimulation and control stimulation (0.2 Hz) were used (*3*). Anesthetized animals were killed 1 minute or 1 hour after delivery of the final stimulus train by application of liquid nitrogen to a retaining cup overlying the cerebral cortex. The regions of the dorsal hippocampus determined to be activated by perforant path stimulation were then dissected at 4°C and used in subsequent biochemical assays. PKC activity in particulate (membrane) and soluble (cytosolic) fractions was then assayed (*10*). In addition, PKC activities were determined after partial protein purification of individual particulate or soluble samples by DEAE-cellulose chromatography, designed to remove substances interfering with the assay of PKC activity (Fig. 1) (*10*).

We observed a twofold increase (relative to low-frequency–stimulated or unoperated controls) in membrane PKC activity 1 hour after LTP stimulation (Fig. 1). Basal kinase activity (measured in the absence of added phospholipid) did not differ significantly between 1-hour LTP and control groups (LTP: 1.13 ±0.09 nmol P_i/min · mg protein; control: 1.25 ± 0.11 nmol P_i/min · mg protein, $n = 19$). The increase in membrane PKC activity was not observed 1 minute after tetanic stimulation; membrane PKC activity in the 1-minute LTP group was similar to both 1-minute and 1-hour low-frequency–stimulated controls as well as unoperated, unstimulated controls (Fig. 1). Thus the increase in membrane PKC activity was not an immediate consequence of high-frequency tetanic stimulation, but required time to develop (*12*).

Along with the increase in PKC activity in the membrane fraction 1 hour after LTP, there was a concomitant decrease in PKC activity in the cytosolic fraction (Fig. 2A). This decrease was nearly equivalent to the increase since the sum total of membrane and soluble PKC activities did not differ significantly between 1-hour LTP and stimulated control groups (Fig. 2B). These alterations in PKC levels after LTP stimulation may be attributed most simply to a redistribution or translocation of PKC activity from the soluble to the particulate phase.

The observed alterations in PKC activity could not be attributed to synaptic transmission per se, since low-frequency stimulation, which evoked more than 300 "population" excitatory postsynaptic potentials and spike responses, did not promote a translocation of PKC activity to membranes (relative to unoperated controls). This suggests that redistribution of PKC activity may be specifically related to the process of enhancement of synaptic transmission initiated by high-frequency repetitive stimulation.

We wished to determine whether the increase in membrane PKC activity, like protein F1 phosphorylation (*5*), was directly related to the regulation of the persistence of synaptic plasticity. PKC activity in the membrane fraction of 1-hour LTP animals was therefore related to the electrophysiological persistence of the enhanced response. This persistence was defined as the percent change in spike amplitude from 1 minute to 1 hour after LTP stimulation. We found that membrane PKC activity was directly related to the persistence of the synaptic enhancement ($r = 0.852$, $P < 0.05$, slope = + 0.42 ± 0.24). Soluble PKC activity, as expected, was inversely related to the persistence of plasticity, but not significantly so ($r = -0.726$; $P < 0.10$, slope = 0.40 ± 0.31). These results indicate that the greater the LTP-induced growth in spike amplitude, the greater the PKC activity in membranes. Interestingly, membrane PKC activity was not related to the percent increase in spike amplitude from pre-LTP to 1 minute or 1 hour after LTP stimulation (1-minute LTP: $r = 0.21$, $P > 0.20$; 1-hour LTP: $r = -0.42$; $P > 0.20$). This supports the suggestion (*5*) that PKC and protein F1

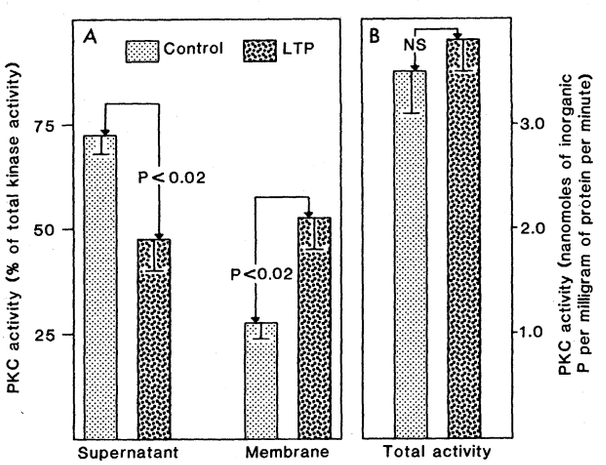

Fig. 2. Translocation of PKC activity by LTP stimulation. Methods were as described in the legend to Fig. 1. All animals were killed 1 hour after LTP. Values are means ± standard errors ($n = 6$ per group).

play an important role in regulating the persistence of the enhanced response but not its amplitude. Since protein F1 appears to be identical to axonal growth-associated proteins [GAP-43 (*13*) and pp 46 (*14*)] and B-50, which is related to PI turnover (*15*), its direct relation to synaptic enhancement (*3, 5*) may require such mechanisms, particularly presynaptic growth (*16*).

The present results suggest a new mechanism for the long-term regulation of synaptic plasticity. The redistribution of PKC activity between membrane and soluble fractions after LTP may indicate that PKC is physically translocated from the cytosol to the membrane. Since ion chelation (with EDTA) was unable to dissociate PKC activity from LTP-stimulated membranes, it is likely that PKC became strongly attached to membranes after LTP. It has been proposed that PKC is activated after its association with the membrane (*17*), and strong attachment of PKC to synaptic membranes could result in prolonged activation following LTP. Increasing the proximity of PKC to its membrane-bound substrates could result in the persistent elevation of substrate phosphorylation, as has been observed with protein F1 phosphorylation 1 hour after LTP (*18*). Consistent with this scenario is the recent observation (*19*) that iontophoretic application of phorbol ester, known to associate PKC with membranes (*10, 11*), enhances the persistence of long-term synaptic plasticity in the dentate gyrus after LTP induction.

REFERENCES AND NOTES

1. D. L. Alkon, *Science* **226**, 1037 (1984); E. R. Kandel and J. H. Schwartz, *ibid.* **218**, 433 (1982); G. Lynch and M. Baudry, *ibid.* **224**, 1057 (1984); A. Routtenberg, *Prog. Neurobiol.* **12**, 85 (1979).
2. A. Routtenberg, in *Neurobiology of Learning and Memory*, G. Lynch, J. McGaugh, N. Weinberger, Eds. (Guilford, New York, 1984), pp. 479–493.
3. ———, D. Lovinger, S. Cain, R. Akers, O. Steward, *Fed. Proc. Fed. Am. Soc. Exp. Biol.* **42**, 755 (1983); A. Routtenberg, D. Lovinger, O. Steward, *Behav. Neural Biol.* **43**, 3 (1985).
4. A. B. Oestreicher, C. J. Van Dongen, H. Zwiers, W. H. Gispen, *J. Neurochem.* **41**, 331 (1983).
5. D. Lovinger *et al.*, *Brain Res.* **343**, 137 (1985).
6. R. Akers and A. Routtenberg, *ibid.* **334**, 147 (1985).
7. R. B. Nelson and A. Routtenberg, *Exp. Neurol.* **89**, 213 (1985).
8. A. Kishimoto, Y. Takai, T. Mori, U. Kikkawa, Y. Nishizuka, *J. Biol. Chem.* **255**, 2273 (1980).
9. M. J. Berridge, *Biochem. J.* **212**, 849 (1983).
10. A. S. Kraft and W. B. Anderson, *Nature (London)* **301**, 621 (1983).
11. M. W. Wooton and R. W. Wrenn, *FEBS Lett.* **171**, 183 (1984).
12. A distinction between early and late events in the development of a plastic change in synaptic communication [B. L. McNaughton, *J. Physiol. (London)* **324**, 249 (1982)] suggests distinct molecular mechanisms, with the increase in membrane PKC activity being related to the later synaptic events underlying long-term synaptic change.
13. J. H. P. Skene and M. Willard, *J. Neurosci.* **1**, 419 (1981).
14. R. B. Nelson, A. Routtenberg, C. Hyman, K. H. Pfenninger, *Soc. Neurosci. Abstr.* **11**, 927 (1985).
15. J. Jolles *et al.*, *Nature (London)* **286**, 623 (1980).
16. A. Routtenberg, *Behav. Neural Biol.* **44**, 186 (1985).
17. Y. Takai, *J. Biol. Chem.* **254**, 3692 (1979).
18. A. Routtenberg *et al.*, *J. Neurochem.* **44**, S135 (1985).
19. D. Lovinger, P. Colley, D. J. Linden, K. Murakami, A. Routtenberg, *Soc. Neurosci. Abstr.* **11**, 927 (1985).

20. This work was supported by National Institute of Mental Health grant MH25281 and Air Force Office of Scientific Research AFOSR 83-0335. We thank Dr. K. Murakami for his assistance and advice.

22 July 1985; accepted 21 October 1985

Equine Infectious Anemia Virus *gag* and *pol* Genes: Relatedness to Visna and AIDS Virus

ROBERT M. STEPHENS, JAMES W. CASEY, NANCY R. RICE*

Comparison of HTLV-III, the putative AIDS virus, with other related viruses, may help to reveal more about the origin of AIDS in humans. In this study, the nucleotide sequence of the *gag* and *pol* genes of an equine infectious anemia virus (EIAV) proviral DNA clone was determined. The sequence was compared with that of HTLV-III and of visna, a pathogenic lentivirus of sheep. The results show that these viruses constitute a family clearly distinct from that of the type C viruses or the BLV–HTLV-I and -II group. Within the family, EIAV, HTLV-III, and visna appear to be equally divergent from a common evolutionary ancestor.

THE FINDING OF GONDA *et al.* (*1*) that cloned genomes of HTLV-III and visna were able to form stable heteroduplexes under conditions of low stringency was the first indication that HTLV-III, the putative cause of human acquired immune deficiency syndrome, should be classified as a lentivirus. Sequence analysis of visna proviral DNA has confirmed this conclusion, revealing that visna is the closest known relative of HTLV-III (*2*). More recent data show that caprine arthritis-encephalitis virus (CAEV), a close relative to visna, also contains regions able to form stable hybrids with HTLV-III DNA (*3*).

Morphologically, equine infectious anemia virus (EIAV) resembles the lentiviruses (*4*); it also shares with them the trait of rapid antigenic variation in the infected host (*5*). Consistent with this classification, a partial cross-reaction between the p24's of lymphadenopathy-associated virus (LAV) and EIAV has been observed (*6, 7*). To determine more precisely the extent to which EIAV is related to HTLV-III, we analyzed the nucleotide sequence of a cloned EIAV proviral genome. Since it is possible to detect even quite distant relatedness if one analyzes highly conserved regions of the genome, we concentrated on the *gag* and *pol* genes.

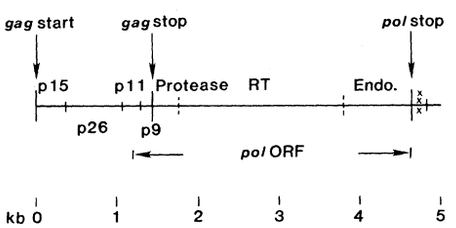

Fig. 1. Proteins encoded by the *gag* and *pol* genes of EIAV. Boundaries between the *gag* proteins are known from the work of Henderson *et al.* (*16*). Boundaries within *pol* are based on homology with other retroviruses and are approximate. In the 180 base pair region immediately downstream of *pol* there are translation terminators in all three reading frames. RT, reverse transcriptase; Endo., endonuclease.

Full-length EIAV proviral DNA was cloned from infected equine fibroblasts (*8*), and after appropriate subcloning the 5′ half of the genome was sequenced by the method of Maxam and Gilbert (*9–11*). The organization of the coding regions is diagrammed in Fig. 1, and the full sequence from the primer binding site (PBS) to the 3′ end of the *pol* gene is shown in Fig. 2.

As in HTLV-III (*12*) and mouse mammary tumor virus (M-MTV) (*13*), the EIAV PBS is complementary to $tRNA_3^{Lys}$, while the visna PBS is complementary to the isoaccepting $tRNA_{1,2}^{Lys}$ (*2*). The two PBS sequences differ at five positions. In contrast, the mammalian type C viruses use $tRNA_{1,2}^{Pro}$ as a primer (*14*) and the avian type C viruses, $tRNA^{Trp}$ (*14*).

Beginning 116 bases after the PBS, there is an eight of nine match with the consensus splice donor sequence (*15*). This is the best

R. M. Stephens and N. R. Rice, LBI–Basic Research Program, Laboratory of Molecular Virology and Carcinogenesis, NCI–Frederick Cancer Research Facility, Frederick, MD 21701.
J. W. Casey, Section of Genetics, Laboratory of Viral Carcinogenesis, National Cancer Institute, Frederick, MD 21701.

*To whom correspondence should be addressed.